

Sensorimotor control during isothermal tracking in *Caenorhabditis elegans*

Linjiao Luo^{1,*}, Damon A. Clark^{1,*}, David Biron^{1,2}, L. Mahadevan^{3,4,†} and Aravinthan D. T. Samuel^{1,†}

¹Department of Physics, Harvard University, Cambridge, MA 02138, USA, ²Department of Biology, Brandeis University, Waltham, MA 02453, USA, ³Division of Engineering and Applied Sciences and ⁴Department of Organismic and Evolutionary Biology, Harvard University, Cambridge, MA 02138, USA

*These authors contributed equally to this work

†Authors for correspondence (e-mail: lm@deas.harvard.edu; samuel@physics.harvard.edu)

Accepted 3 October 2006

Summary

In order to purposefully navigate their environments, animals rely on precise coordination between their sensory and motor systems. The integrated performance of circuits for sensorimotor control may be analyzed by quantifying an animal's motile behavior in defined sensory environments. Here, we analyze the ability of the nematode *C. elegans* to crawl isothermally in spatial thermal gradients by quantifying the trajectories of individual worms responding to defined spatiotemporal thermal gradients. We show that sensorimotor control during isothermal tracking may be summarized as a strategy in which the worm changes the curvature of

its propulsive undulations in response to temperature changes measured at its head. We show that a concise mathematical model for this strategy for sensorimotor control is consistent with the exquisite stability of the worm's isothermal alignment in spatial thermal gradients as well as its more complex trajectories in spatiotemporal thermal gradients.

Supplementary material available online at
<http://jeb.biologists.org/cgi/content/full/209/23/4652/DC1>

Key words: *C. elegans*, thermotaxis, sensorimotor control.

Introduction

The goal of systems neuroscience is to understand animal behavior in terms of transformations of sensory input into motor output that are specified and carried out by the intact nervous system. One advantage of studying simple animals like the nematode *Caenorhabditis elegans* is that certain patterns of sensorimotor transformation can be vividly displayed in the animal's stereotyped movements in defined sensory environments. The simplicity of the 302-neuron nervous system of *C. elegans* means that descriptive models of sensorimotor transformation that are established at the level of animal behavior may eventually be mapped to mechanistic models at the level of the nervous system (White et al., 1986). In order to be useful, descriptive models of behavior must compactly and accurately represent the animal's behavior in terms of distinct input–output relationships that facilitate mapping to the basic operations of neuronal circuits.

The best understood sensorimotor behaviors in *C. elegans* are reflexive avoidance to body touch (Chalfie et al., 1985), its chemotactic ability to crawl up and down chemical gradients (Bargmann and Horvitz, 1991), and its thermotactic ability to descend thermal gradients in what is called cryophilic movement (Hedgecock and Russell, 1975). When *C. elegans* is

touched on its head or tail, it reflexively crawls backward or forward with propulsive undulations (Chalfie et al., 1985). When the animal crawls up or down chemical or thermal gradients, it tends to extend (shorten) periods of forward movement by reducing (increasing) the stochastic occurrence of reorientation maneuvers in response to improving (declining) conditions. This biased-random walk strategy leads to net migration towards favored environments (Pierce-Shimomura et al., 1999; Ryu and Samuel, 2002). The systematic analysis of neuronal lesions in *C. elegans* that disrupt touch avoidance or change the occurrence of reorientation maneuvers has uncovered parts of the *C. elegans* nervous system that contribute to the sensorimotor transformations of their respective behaviors (Chalfie et al., 1985; Tsalik and Hobert, 2003; Wakabayashi et al., 2004; Gray et al., 2005).

C. elegans also has the ability to track isotherms in spatial thermal gradients when it navigates at temperatures near its previous cultivation temperature (Hedgecock and Russell, 1975). Although isothermal tracking behavior in *C. elegans* has been known for 30 years, the sensorimotor strategy that allows the worm to actively maintain isothermal alignment in spatial thermal gradients has not been characterized. Unlike the biased random walk strategy that characterizes cryophilic movement

down thermal gradients, the isothermal tracking behavior is strikingly deterministic: an individual animal strays from each isothermal track by $<0.1^{\circ}\text{C}$ over prolonged periods of forward movement (Hedgecock and Russell, 1975; Ryu and Samuel, 2002). Although the isothermal tracking behavior is often used as a metric of thermotactic memory (e.g. Gomez et al., 2001; Biron et al., 2006), how *C. elegans* transforms thermosensory perception of the surrounding thermal gradient into deterministic patterning of its own movements is not known. Here, we characterize sensorimotor control in isothermal tracking by quantifying the trajectories of individual animals navigating defined spatiotemporal thermal gradients, and offer a minimal mathematical model of the sensorimotor transformation at the behavioral level that is consistent with experimental observations.

Materials and methods

Strain

The wild-type *Caenorhabditis elegans* N2 strain and the mutant *ttx-3(ks5)* and *ttx-4(nj1)* strains were obtained from the *C. elegans* Genetics Center (Minneapolis, MN, USA), and were cultivated at 20°C using standard methods (Brenner, 1974).

Isothermal tracking assays

In each assay, 20–25 young adult worms were washed in NGM buffer for ~ 1 min before being moved to a 9-cm NGM agar plate (Sulston and Hodgkin, 1988). The plate was then placed on an aluminum surface under thermoelectric control (Ryu and Samuel, 2002). Linear thermal gradients were established by separately controlling the temperature at the ends of a rectangular aluminum surface. Radial thermal gradients were established by separately controlling the temperature of a copper pin at the center of an aluminum disk and the temperature of the disk's perimeter. Worms were illuminated by a ring of superbright LEDs. Video was captured using a CCD camera for 30 min at 0.5 frames s^{-1} using LabVIEW (National Instruments, Austin, TX, USA). We used low magnification (10 cm across a video frame) to characterize the trajectories of individual animals on spatial thermal gradients and at higher magnification (2 cm across a video frame) to quantify the wavelength, speed and undulation frequency during isothermal tracking. Video was analyzed using particle-tracking and analysis algorithms written in MATLAB (Mathworks, Natick, MA, USA) (Crocker and Grier, 1996). Separate custom-written software for population-wide behavioral quantification enabled us to simultaneously monitor and analyze the movements of 20–40 worms navigating each spatial thermal gradient. In order to detect isothermal tracks, the software decomposed the trajectory of each worm into runs and turns, and scored each track as a run deviating from isothermal alignment by less than $<0.1^{\circ}\text{C}$.

Superposed temporal variation

Agar surfaces were heated and cooled in a spatially uniform manner by feedback controlled illumination from a heat lamp

held 1 m above the surface. Temperature was monitored at the surface of the plate using a small thermocouple (0.2 mm, Physitemp Instruments, Clifton, NJ, USA), which then regulated voltage to the heat lamp with a PID feedback loop operating on a computer running LabVIEW (National Instruments).

Simulations

Numerical simulations of the model represented by Eqn 2 and Eqn 3 were carried out using standard integration packages in MATLAB.

Results

Isothermal tracks are prolonged periods of forward movement

First, we quantified the temperatures and durations of isothermal tracks of *C. elegans* navigating fixed spatial thermal gradients at temperatures near their previous cultivation temperature by using a computerized tracking system that allowed us to simultaneously monitor and analyze the movements of large populations of worms (see Materials and methods). We verified that an individual worm may track any isotherm within 2°C of its prior cultivation temperature – *C. elegans* cultivated at 20°C will track isotherms between 18 and 22°C – suggesting that the worm is less concerned about choosing the temperature of each isotherm than it is about maintaining isothermal alignment after it has started each track (Fig. 1A,B; Movie 1 in supplementary material) (Ryu and Samuel, 2002). When tracking a specific isotherm, *C. elegans* deviates from that isotherm by about 0.1°C . We quantified the percentage of time that an individual worm spends tracking isotherms by quantifying the total duration of all isothermal movements exhibited by populations of *C. elegans* navigating gradients of defined steepness in 30 min. Thus, we found that on gradients $>0.2^{\circ}\text{C cm}^{-1}$ in steepness, *C. elegans* spends ~ 15 – 20% of its time tracking isotherms, and the rest of its time moving randomly in other directions in the intervals preceding and following each isothermal track (Fig. 1C). The tendency to move isothermally is reduced on spatial thermal gradients shallower than $\sim 0.1^{\circ}\text{C cm}^{-1}$, which appears to represent the threshold steepness for the behavior (Fig. 1C).

The start and end of each isothermal track are marked by sudden reorientation maneuvers (abrupt turns or reversals followed by abrupt turns), which provide and disrupt isothermal alignment, respectively. Using radial thermal gradients with a defined steepness of 0.2 – $1.3^{\circ}\text{C cm}^{-1}$, we found that the durations of isothermal tracks are exponentially distributed and on average about 80 s long. In other words, the statistics of terminating an isothermal track are Poisson: during each second of an isothermal track, *C. elegans* has a 1.25% likelihood of terminating the track by spontaneously reorienting itself with an abrupt turn or reversal (Fig. 1D). In contrast, the mean duration of each run exhibited by *C. elegans* navigating an isotropic environment at 20°C is approximately 20 s (or 5% chance of termination per second) (Fig. 1E). Therefore, when *C. elegans* is tracking an isotherm,

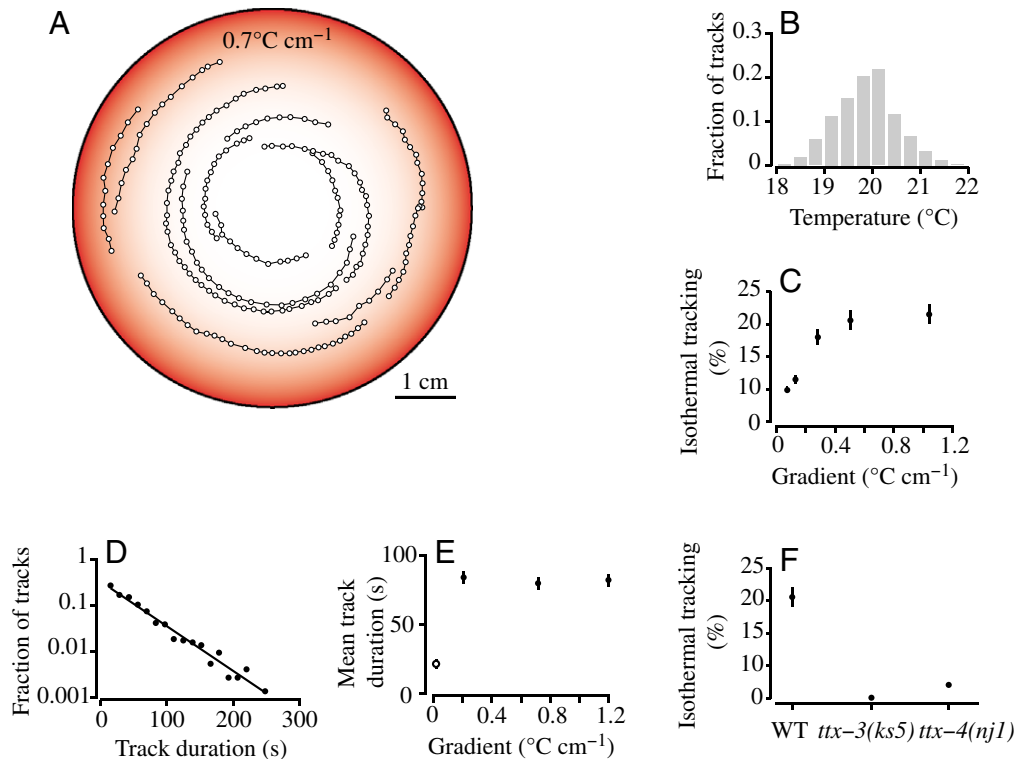


Fig. 1. Isothermal tracks. (A) Representative isothermal tracks of wild-type worms (N2 strain) cultivated at 20°C navigating a radial thermal gradient on the surface of a 9-cm diameter agar plate. The temperature from center to edge is 18.5 to 21.5°C , corresponding to $0.7^{\circ}\text{C cm}^{-1}$ steepness. The trajectory of each isothermal track on the spatial gradient is shown by open circles connected by black lines, with each circle indicating position of the worm centroid at 10 s intervals throughout each track. For purposes of presentation, the undirected movements before and after each isothermal track are not shown. (B) Histogram of the absolute temperatures of ~ 400 isothermal tracks made by wild-type worms cultivated at 20°C navigating linear thermal gradients from 15 – 25°C . (C) Percentage of time spent in isothermal movement of wild-type worms navigating defined spatial thermal gradients, quantified for each data point by totaling the duration of each isothermal movement exhibited by 60 worms in 30 min of observation on linear thermal gradients, and then dividing by 1800 min. Error bars represent ± 1 s.e.m. (D) Histogram of the durations of ~ 400 isothermal tracks made by wild-type worms navigating a radial thermal gradient with $0.7^{\circ}\text{C cm}^{-1}$ steepness. The solid line shows a fit to an exponential function ($\tau=80$ s; $P>0.5$). (E) Mean durations of isothermal tracks of wild-type worms navigating radial spatial thermal gradients with 0.2 , 0.7 , and $1.2^{\circ}\text{C cm}^{-1}$ steepness (black circles). Each point represents data from ~ 400 tracks. For comparison, the mean duration of ~ 1000 runs exhibited by wild-type worms navigating an isotropic environment at 20°C is also shown (open circle at $0^{\circ}\text{C cm}^{-1}$). Error bars represent ± 1 s.e.m. (F) Percentage of time spent in isothermal movement of wild-type (WT) and mutant worms navigating spatial thermal gradients with 0.5°C steepness, quantified for each data point by totaling the duration of each isothermal movement exhibited by 60 worms in 30 min of observation on linear thermal gradients, and then dividing by 1800 min. Error bars represent ± 1 s.e.m.

it strongly suppresses the occurrence of abrupt reorientation maneuvers.

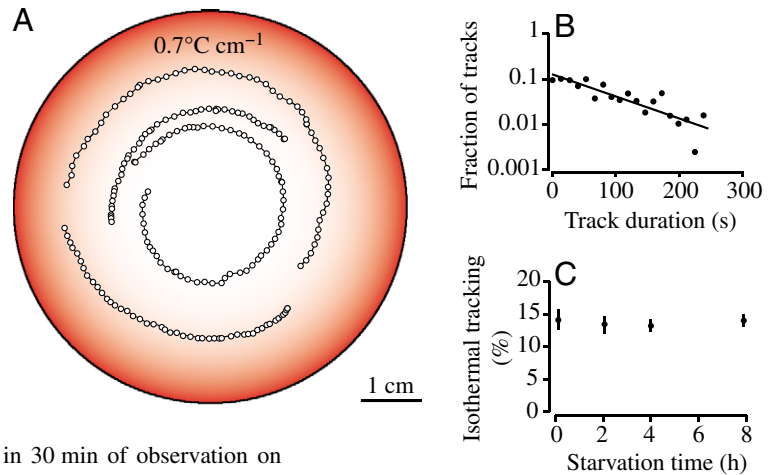
The *ttx-3* and *ttx-4* mutations cause *C. elegans* to accumulate at the coldest points and warmest points on spatial thermal gradients, and are called cryophilic and thermophilic phenotypes, respectively. The *ttx-3* gene encodes a LIM homeobox gene that is required for normal development of the AIY interneuron (Hobert et al., 1997). The *ttx-4* gene encodes a protein kinase C that is broadly expressed in *C. elegans* sensory neurons, including the AFD thermosensory neuron (Okochi et al., 2005). We found that both mutations severely disrupt the ability of *C. elegans* to track isotherms near the temperature of its previous cultivation (Fig. 1F). This observation suggests that isothermal tracking behavior may be particularly fragile with respect to genetic mutations that affect thermosensation, as in order for *C. elegans* to track isotherms

for extended periods of time, the worm must be able to detect both positive and negative temperature fluctuations from isothermal alignment with exquisite sensitivity and reliability.

Isothermal tracking occurs in the presence of bacterial food and is unaffected by starvation

Since *C. elegans* only tracks isotherms near its previous cultivation temperature, this form of long-term experience-dependent plasticity is often assumed to reflect an associative link between the presence of bacterial food and a particular temperature (Hedgecock and Russell, 1975; Mohri et al., 2005). Recently, we found that this form of thermotactic plasticity does not, in fact, require food; sustained exposure to a new temperature without food leads to isothermal tracking near the new temperature (Biron et al., 2006). In this study, we found that *C. elegans* also tracks isotherms in the presence of bacterial

Fig. 2. The effect of food and starvation on isothermal tracking. (A) Representative isothermal tracks of wild-type worms navigating radial thermal gradients with uniformly spread bacterial lawns. The temperature from center to edge of the plate was 18.5 to 21.5°C, corresponding to a steepness of 0.7°C cm⁻¹. The time interval between data points is 10 s. (B) Histogram of the durations of isothermal tracks of wild-type worms navigating a radial thermal gradient with 0.7°C steepness in the presence of bacterial lawns. The solid line shows a fit to an exponential ($\tau=156\pm 6$ s; $P>0.2$). (C) Percentage of time spent in isothermal movement of wild-type navigating spatial thermal gradients with 0.5°C cm⁻¹ steepness, after overnight cultivation at 20°C with bacterial food and being placed at 20°C without food for fixed periods of time. Each data point was quantified by totaling the duration of each isothermal movement exhibited by 60 worms in 30 min of observation on linear thermal gradients, and dividing by 1800 min. Error bars represent ± 1 s.e.m.



food (Fig. 2A). The average duration of isothermal tracks of *C. elegans* crawling on spatial thermal gradients in bacterial lawns is actually longer than that in the absence of food (Fig. 2B). In order to test whether starvation affects the ability to track isotherms, we cultivated *C. elegans* at 20°C, and then starved them at 20°C for fixed periods of time. We then allowed these starved worms to navigate spatial thermal gradients near 20°C, and counted the number of isothermal tracks that they exhibited in a fixed interval of time. We found no significant variation in the number of isothermal tracks exhibited after starvation for as long as 8 h (Fig. 2C). We conclude that the presence or absence of food has limited relevance to isothermal tracking. Instead, isothermal tracking might simply be a homeostatic mechanism; moving to new temperatures is likely to require adaptation in the rates of numerous biochemical and metabolic pathways, an expense that can be avoided by tracking isotherms.

Isothermal tracks are not preceded by deterministic movement

Isothermal tracks are usually preceded and followed by long periods of undirected movement, in which successive runs fail to be oriented along isotherms. We asked whether the movement of individual animals in the time interval preceding each isothermal track is stereotyped, which would provide evidence for deterministic pursuit of isothermal alignment. We quantified the direction and duration of the preceding runs of each isothermal track exhibited by *C. elegans* navigating a linear thermal gradient (Fig. 3A). We found that neither the direction nor the duration of the preceding runs are correlated with the direction of the subsequent track, although the size of the reorientation maneuver that separates the preceding run from the subsequent isothermal track tends to be $<90^\circ$ (Fig. 3B). Although isothermal alignment appears to be initially serendipitous, the alignment is thereafter actively maintained, as exhibited in the radial gradient assays. In rare but striking cases, worms terminate one isothermal track and rapidly begin tracking a different isotherm; the intervening time interval between two different isothermal tracks can be as little

as 10 s (Fig. 3C). Therefore, isothermal tracking does not appear to reflect commitment to, or long-term memory of, the absolute temperature of each isotherm. Instead, it appears that each isothermal track is begun anew when a reorientation maneuver serendipitously provides isothermal alignment. The strategy for isothermal tracking allows the worm to maintain isothermal alignment once it is found, but not to pursue isothermal alignment. This observation also suggests that the long-term memory of cultivation temperature is actually represented by the range of temperatures in which a worm may track isotherms (e.g. the distribution depicted in Fig. 1B), not by the specific temperatures of each isotherm that an individual might track.

Isothermal tracking does not affect the speed or wavelength of propulsive undulations

Although the mechanism for isothermal tracking behavior appears to primarily work by steering the direction of forward movement, it may also affect other physiological parameters of the propulsive undulations that drive forward movement. Using video microscopy, we quantified the propulsive undulations of *C. elegans* freely crawling on an agar surface at 20°C and of *C. elegans* tracking isotherms on spatial thermal gradients with defined steepness (Fig. 4A). However, we found no measurable differences in the wavelength or frequency of propulsive undulations between freely crawling and isothermally tracking animals (Fig. 4B,C). Also, the center-of-mass speed of freely crawling worms and isothermally tracking worms is approximately the product of the wavelength and the frequency of the propulsive undulations, suggesting that the worm's body slides longitudinally along its sinusoidal path with little lateral slip (Fig. 4C). Taken together, these data suggest that the mechanism for isothermal tracking works by steering the forward movement of the worm's head in response to sensory inputs, but that this steering mechanism does not significantly change the baseline bodily mechanics that provide propulsion.

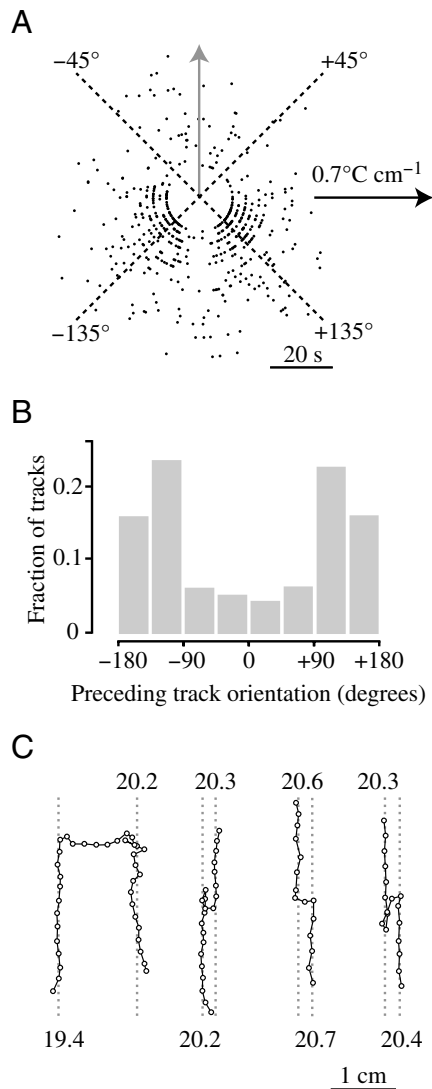


Fig. 3. Movement preceding isothermal tracks. (A) Scatter plot indicating the duration and direction of the run preceding each isothermal track of wild-type worms navigating a linear thermal gradient with $0.7^{\circ}\text{C cm}^{-1}$ steepness. Black arrow indicates direction of the thermal gradient. For presentation purposes, the start points of all isothermal tracks are centered at the origin, and the isothermal tracks corresponding to each data point are aligned to the direction of the gray arrow. Black circles indicate the start point of the run preceding each isothermal track relative to the start-point of that isothermal track. Radial distance from the origin represents the duration of the preceding run (see scale bar), and the orientation is indicated by the angle with respect to the directions of the linear thermal gradient. Data corresponding to ~ 700 isothermal tracks are shown. Preceding runs <10 s in duration are excluded. (B) Histogram of the orientation of the run preceding each isothermal track, using data from Fig. 2A. The dip at 0° indicates that isothermal tracks are not typically preceded by runs with strong isothermal alignment in the opposite direction. Also, the dip at 180° indicates that preceding runs closely aligned with the isothermal track tend to be categorized as part of the same isothermal track. (C) Representative trajectories of *C. elegans* that left one isothermal track and rapidly began tracking a new isotherm at a different temperature. Open circles indicate worm centroid position at 5 s intervals.

Movements of *C. elegans* in spatial thermal gradients with shallow superposed temporal gradients

In order to uncover the elements of sensorimotor control that allow *C. elegans* to steer its own forward movement during isothermal tracking, we analyzed the individual trajectories of populations of worms navigating radial thermal gradients with fixed spatial steepness while applying a temporal thermal gradient in a spatially uniform manner – on

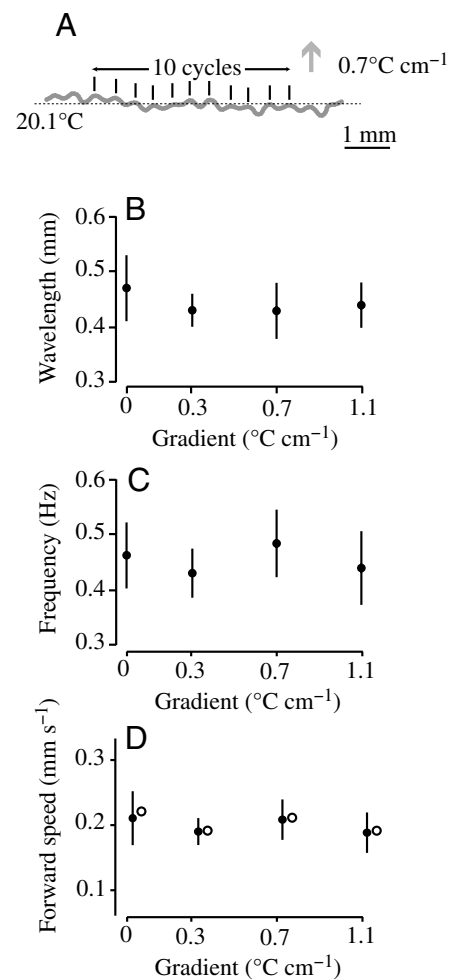


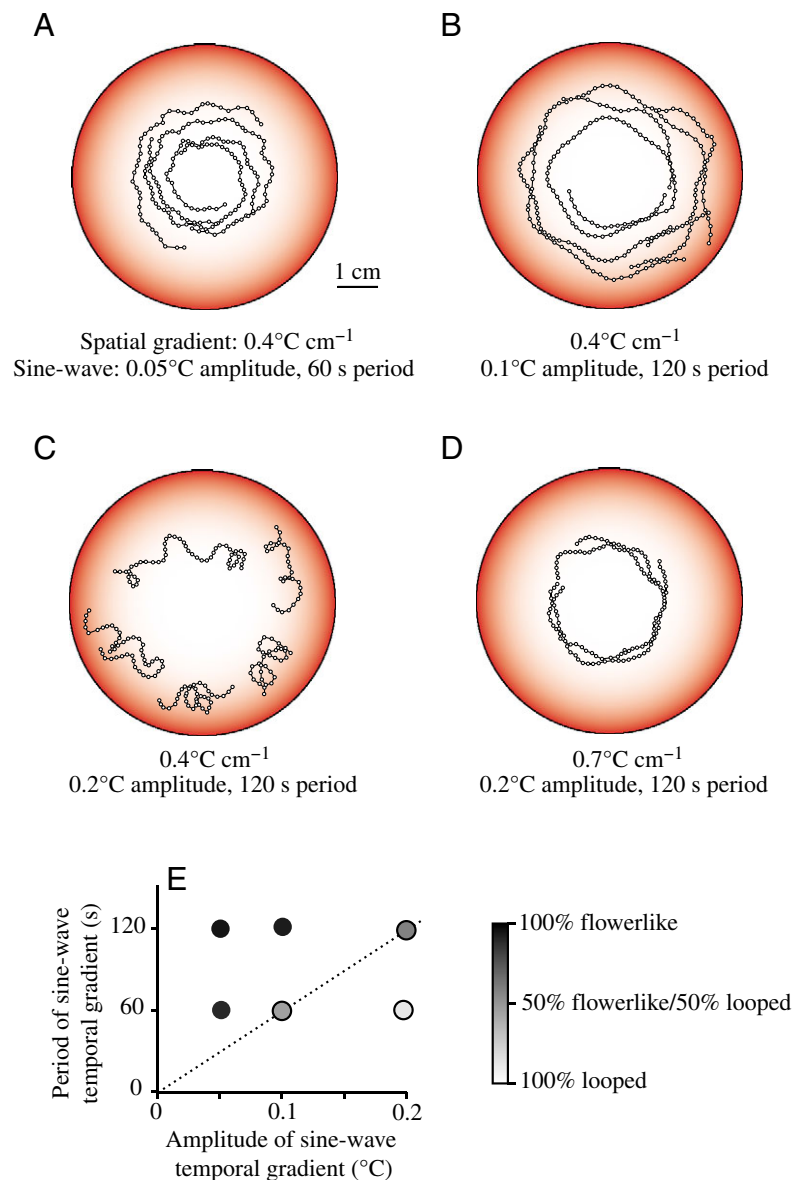
Fig. 4. Isothermal tracking does not affect the speed, wavelength, or frequency of propulsive undulations. (A) Using video microscopy, we quantified the propulsive undulations of *C. elegans*. Here, we show the representative path traced by the head of a worm crawling along an isotherm near 20.1°C on a spatial thermal gradient with $0.7^{\circ}\text{C cm}^{-1}$ steepness. Based on the video images and movies of *C. elegans* crawling freely on agar surfaces and tracking defined spatial thermal gradients, we quantified the wavelength of sinusoidal bending (B), the temporal frequency of the propulsive undulation (C), and the center-of-mass speed of the movement of the animal's body. In (D), black circles represent direct measurements of the center-of-mass speed, and the white circles are the product of the wavelength and frequency measurements from (B) and (C). Each data point corresponds to measurements with 20 animals. Error bars represent ± 1 s.d., which reflect the worm-to-worm variabilities in the speed and geometry of propulsive undulations.

top of the spatial gradient, we superposed sine-wave temporal variation in temperature with defined amplitude (T_0) and angular frequency (Ω). In this setup, each isotherm corresponds to a circle contracting and expanding in time. We found that when *C. elegans* navigates these spatiotemporal thermal gradients, it follows the moving isotherms, producing florally patterned trajectories (Fig. 5A). We found that increasing the amplitude and period of the applied temporal sine-wave increases the size and spacing of the floral petals, respectively (Fig. 5B). These observations indicate that *C. elegans* uses temporal sensory processing to track isotherms. If *C. elegans* responded directly to the spatial gradient – e.g. by minimizing a spatial difference in temperature measured instantaneously at its head and tail – then it would continue to track circles on radial spatial gradients, as long as any temporal changes in the temperature of its environment were spatially uniform.

Movements of C. elegans in spatial gradients with steep superposed temporal gradients

Thermosensory input in *C. elegans* is likely to occur at the front of its head, at the sensory endings of neuronal dendrites like those of the AFD thermosensory neuron (Perkins et al., 1986; Cassata et al., 2000; Satterlee et al., 2001; Clark et al., 2006). When *C. elegans* crawls in a spatial thermal gradient, a thermoreceptor at the head measures an oscillating thermosensory input driven by the worm's undulating gait and side-to-side movements. Isothermal alignment in a spatial thermal gradient then implies that the thermosensory input will oscillate with warming and cooling phases that are equal and opposite, and the time-derivative of the measured temperature changes will be $\nabla T \cdot v$, where ∇T is the steepness of the ambient spatial gradient and v is the instantaneous velocity of the worm's head. The simplest strategy that utilizes temporal sensory processing to maintain isothermal alignment is for the

Fig. 5. Spatiotemporal thermal gradients. Representative trajectories of worms navigating spatiotemporal thermal gradients with fixed steepness in the radial direction and with superposed, spatially uniform, sine-wave temporal variation. Each trajectory shows a single period of persistent forward movement exhibited by a worm navigating these gradients, with positions along each run indicated at 10 s intervals. (A) When worms navigate a spatiotemporal thermal gradient with $0.4^\circ\text{C cm}^{-1}$ spatial steepness and sine-wave temporal variation with 0.05°C amplitude and 60 s period, prolonged floral trajectories emerge as the worm follows each isotherm during cycles of contraction and expansion. (B) Floral trajectories of worms navigating a spatiotemporal thermal gradient with $0.4^\circ\text{C cm}^{-1}$ spatial steepness and sine-wave temporal variation with 0.1°C amplitude and 120 s period. (C) Floral trajectories are largely replaced by looping trajectories when worms navigate a spatiotemporal thermal gradient with $0.4^\circ\text{C cm}^{-1}$ spatial steepness and sine-wave temporal variation with 0.2°C amplitude and 120 s period. (D) Floral trajectories of worms navigating a spatiotemporal thermal gradient with the same temporal variation as in Fig. 4C, but with a 0.7°C spatial steepness. (E) The relative appearance of floral and looping trajectories on spatiotemporal gradients with fixed $0.4^\circ\text{C cm}^{-1}$ spatial steepness depends on the steepness of the superposed temporal gradient. The steepness of the temporal gradient is proportional to its amplitude (T_0) and frequency (Ω). The floral trajectories dominate when ΩT_0 is small (above the dotted line), and are replaced by looping trajectories when ΩT_0 is large (below the dotted line). The shading of each circle corresponds to the fraction of floral trajectories in a dataset corresponding to ~ 300 tracks. The dotted line indicates the approximate boundary between loop-like and flower-like trajectories, occurring as α approaches 1; the dotted line shows $\alpha \sim 0.4$.



worm to actively strive to balance the warming and cooling phases of the thermosensory input. Indeed, imposing temporal variations on the environment that are comparable to or exceed the temporal variations driven by self-movement in the spatial gradient allows us to test if such a strategy is at work.

In the experiments shown in Fig. 5A,B, the maximum rate of temperature change imposed on the environment ($\Omega T_0 \sim 0.005^\circ\text{C s}^{-1}$, where Ω is the imposed frequency and T_0 is the imposed amplitude) is less than the maximum rate of temperature change driven by self-movement of the head on those spatial gradients ($|v|\nabla T \sim 0.012^\circ\text{C s}^{-1}$), which allows the worm to follow the moving isotherms in stable floral trajectories. In Fig. 5C, we show the results of an increase in the rate of imposed temperature variation to $\Omega T_0 \sim 0.010^\circ\text{C s}^{-1}$, which disrupts the floral trajectories as they begin to loop back on themselves. Note that these loops are still approximately isotherms. In Fig. 5D, we show that increasing the steepness of the spatial gradient restores the floral trajectories by increasing the temporal variations driven by self-movement. We quantified the relative occurrence of floral trajectories and looping trajectories of worms navigating spatial gradients with $0.4^\circ\text{C cm}^{-1}$ steepness and with sine-wave temporal variations with different periods and amplitudes. We found that the boundary between the two types of trajectories in terms of the parameters of the spatiotemporal thermal gradients occurs when ΩT_0 and $|v|\nabla T$ are comparable, which is consistent with a model of temporal processing of thermosensory input.

Although floral pattern trajectories and looping trajectories are visibly distinguishable, they may be different instantiations of the same sensorimotor transformation, executed in different parameter spaces of the spatiotemporal thermal gradient. During either type of trajectory, *C. elegans* actively steers the direction of its forward movement in response to thermosensory input. The absence of abrupt reorientation maneuvers during isothermal tracking suggests that the worm must be actively and continuously modulating the curvature of its propulsive undulations during isothermal tracking. When *C. elegans* has perfect isothermal alignment, thermosensory input at the head will have perfectly balanced warming and cooling phases. However, any deviation from isothermal alignment will produce an asymmetry in the warming and cooling phases of the thermosensory input, which the worm could exploit, in principle, as an error signal to correct isothermal alignment. The simplest hypothesis is that the worm maintains isothermal alignment by responding to any temporal change in the thermosensory input driven by its own movement by countering that movement, an action that may be achieved by increasing the curvature of the trajectory of the head.

Mathematical modeling of sensorimotor control in isothermal tracking

Since *C. elegans* crawls by undulating with negligible lateral slipping, it is possible to approximate its forward movement with mathematical conciseness, by using a single-scalar quantity to describe the time-varying curvature of the worm's head, which determines the subsequent path of the body. Upon

this framework, we build a minimal phenomenological model for isothermal tracking as a direct transformation between thermosensory input and the curvature of forward undulatory movement. We note that the simplifying assumption of negligible lateral slip does not apply to all types of agar surfaces. In many cases the slipping of the body of *C. elegans* slows its forward speed by up to 20% relative to a no-slip condition (Karbowksi et al., 2006).

With the simplifying assumption of negligible lateral slip, the entire undulating path of *C. elegans* sliding at speed $|v|$, within each persistent period of forward movement, is completely described by one variable $\theta(t)$, the angle of the tangent to the worm's head with respect to a fixed axis in the plane, which we define so that $\theta = \pi/2$ when the head is pointing directly up the spatial gradient. The undulating path can also be described in terms of the time-varying curvature at the worm's head, $\kappa(t) = \dot{\theta}/v$. Therefore, a model of a crawling *C. elegans* during each isothermal track only needs to take one mathematical conversion into account, between changes in thermosensory input at the head (\dot{T}) and changes in curvature at the head (proportional to $\ddot{\theta}$).

Even in the absence of any temperature gradients, $\dot{T} = 0$, *C. elegans* crawls with propulsive undulations with basal frequency ω and amplitude θ_0 , so that we model its motion as a simple oscillator that is determined by:

$$\ddot{\theta} = \theta_0 \omega^2 \sin \omega t, \quad (1)$$

where $(\dot{\ }) = d(\)/dt$. Our minimal descriptive model of isothermal tracking behavior contends that *C. elegans* simply curves more vigorously to in response to any temporal change in the thermosensory input (Fig. 6A). This strategy may be incorporated by using a multiplicative factor in Eqn 1, allowing *C. elegans* to change its curvature in proportion to changes in the thermosensory input, \dot{T} :

$$\ddot{\theta} = \theta_0 \omega^2 (\sin \omega t) [1 + f(\dot{T})]. \quad (2)$$

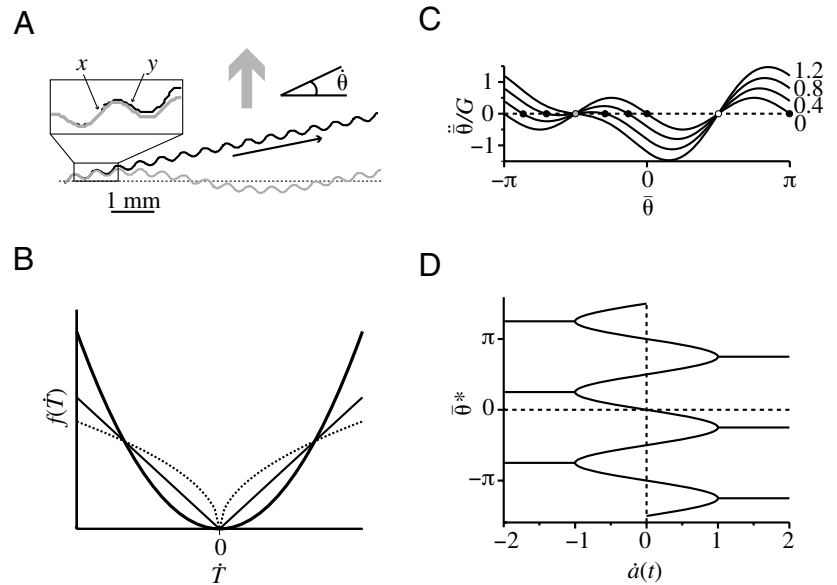
The functional form of $f(\dot{T})$ is dictated by considerations of symmetry, and minimally demands that a change in the sign of \dot{T} (i.e. inverting the temperature gradient) does not affect the response, i.e. $f(\dot{T}) = f(|\dot{T}|)$. In this discussion, we focus on the case $f(\dot{T}) = g\dot{T}^2$, where g is a scalar gain, for its analytical simplicity. A wide variety of functional forms – e.g. those that are shown in Fig. 6A, can produce qualitatively similar results in numerical simulations.

In our experiments, the thermosensory input in a spatiotemporal thermal gradients depends on (a) the amplitude and frequency of the superposed temporal thermal gradient, (b) the speed and direction of the worm's head, and (c) the steepness of the ambient spatial thermal gradient, so that:

$$\begin{aligned} \dot{T} &= T_t + v \cdot \nabla T \\ \dot{T} &= T_0 \Omega \cos(\Omega t) + |v| |\nabla T| \sin[\theta(t)], \end{aligned} \quad (3)$$

where $(\dot{\ }) = \partial(\)/\partial t$. At this point, the pair of coupled non-linear differential equations, Eqn 2 and Eqn 3 and the functional form of $f(\dot{T})$, provide a full description of the dynamical system

Fig. 6. Analysis of the mathematical model. (A) Worm trajectories calculated using the model represented by Eqn 2 and Eqn 3 with and without a spatial thermal gradient. The black arrow indicates the direction of worm movement, the thick grey arrow indicates the direction of the thermal gradient, and the dotted line indicates an isotherm. The black line is the calculated trajectory without the gradient. The grayed trajectory shows the calculated trajectory in response to the perturbation caused by the gradient. The two labeled points in the magnified region indicate the extrema of both $\theta(t)$ and $\bar{\theta}(t)$. At point x , $|\dot{T}|^2$ is greater than at point y , so the worm curves more vigorously at x , leading to a slight right turn that corrects isothermal alignment. (B) Functional forms of $f(\dot{T})$, all of which can generate calculated trajectories consistent with the movements of real *C. elegans* responding to spatiotemporal thermal gradients. The requisite feature for the qualitative behavior is that $f(\dot{T})$ is monotonic in $|\dot{T}|$. The thick line corresponds to the function $f(\dot{T})=g|\dot{T}|^2$, the functional form we use in the analytical discussion in Results. (C) Plot of $\ddot{\theta}/G$ as a function of $\bar{\theta}$ and $\dot{\alpha}(t)$. The values of $\dot{\alpha}(t)$ are listed to the right of their curves. Black dots represent stable fixed points, the white dot represents an unstable point, and the gray circle switches from unstable to stable when $\dot{\alpha}(t)>1$. (D) Plots of the fixed point $\bar{\theta}^*$ as a function of $\dot{\alpha}(t)$. When $\dot{\alpha}(t)$ undergoes small oscillations about 0, so does $\bar{\theta}^*$. When $\dot{\alpha}(t)$ approaches 1, the fixed point is able to move to different branches of the graph, corresponding to the looped trajectories exhibited by *C. elegans* responding to steep superposed temporal gradients.



corresponding to the moving animal. All parameters that we used in the model are summarized in Table 1. We performed numerical simulations of Eqn 2 and Eqn 3, fitting g to the experimental observations of Fig. 5, and found that we were able to reproduce the basic dynamics of real worms navigating the spatiotemporal thermal gradients in the range of our experiments (Fig. 7A–D).

Furthermore, several considerations allow us to develop an approximate analytical solution to the model for sensorimotor control represented by Eqn 2 and Eqn 3. First, we are less interested in the detailed behavior of the tangent to the worm's head (the parameter θ) than in the overall averaged heading of the animal ($\bar{\theta}$) in response to spatiotemporal thermal gradients defined as:

$$\bar{\theta} = \frac{1}{2\pi/\omega} \int_0^{2\pi/\omega} \theta(t) dt,$$

where $2\pi/\omega$ is the period of undulation. Second, we know that $\bar{\theta}$ changes very little over single undulation cycles, allowing us

to analyze changes in $\bar{\theta}$ as first-order perturbations. Third, in our experiments, we provide our temporal gradients with slow frequencies ($\Omega \ll \omega$), so we are mainly interested in the limit in which the superposed temporal thermal gradients can be viewed as constant in time with respect to the faster oscillations driven by self-movement. We begin by integrating Eqn 2 over the period of one undulation cycle ($T=2\pi/\omega$), noting that the first term vanishes immediately:

$$\begin{aligned} \ddot{\bar{\theta}} &= \frac{1}{2\pi/\omega} \int_0^{2\pi/\omega} \ddot{\theta} dt \\ &= \frac{\theta_0 \omega^2}{2\pi/\omega} \int_0^{2\pi/\omega} \sin(\omega t) f(\dot{T}) dt. \end{aligned} \quad (4)$$

In order to integrate Eqn 4, we must incorporate Eqn 3 that describes changes in the thermosensory input, \dot{T} , which is a function of the movement of the worm's head and of time. Since the superposed temporal variations that characterize our experiments are slow with respect to the undulation cycle and

Table 1. Parameters used in numerical simulations of the mathematical model

Parameter	Source	Typical value
$2\pi/\omega$, undulation period of crawling worm	Observation	2 s
$ v $, instantaneous velocity of the worm's head	Observation	0.03 cm s ⁻¹
θ_0 , maximum angle of head with respect to average heading, $\bar{\theta}$	Observation	$\pi/4$
$2\pi/\Omega$, period of imposed sine-wave temporal thermal gradient	Experimentally controlled	60–120 s
T_0 , amplitude of superposed sine-wave temporal thermal gradient	Experimentally controlled	0–0.4°C
∇T , steepness of superposed spatial thermal gradient	Experimentally controlled	0–0.7°C cm ⁻¹
g , gain on $ \dot{T} ^2$ in $f(\dot{T})$	Free parameter of model	~200 s ² °C ⁻²

the fast variations in temperature are driven by the movements of the worm's head in the spatial thermal gradient, we may employ a perturbative expansion of $f(\bar{T})$ about the mean direction of the animal's head, $\bar{\theta}$. This allows us to calculate the first non-vanishing integrated term:

$$\ddot{\bar{\theta}} = -\frac{1}{2}\theta_0^2\omega^2 \frac{df(\bar{T})}{d\bar{\theta}}. \quad (5)$$

Finally, for the case $f(\bar{T})=g\bar{T}^2$, Eqn 5 yields the ordinary differential equation:

$$\ddot{\bar{\theta}} = -G\cos(\bar{\theta})[\sin(\bar{\theta}) + \dot{\alpha}(t)] \quad (6)$$

for the averaged orientation variable $\bar{\theta}$ driven by a scaled temperature gradient:

$$\dot{\alpha}(t) = \frac{T_0\Omega\cos(\Omega t)}{|v||\nabla T|},$$

that governs the relative contributions of the superposed temporal gradient and the temporal gradient associated with locomotion. Here $G=g\theta_0^2\omega^2|v|^2|\nabla T|^2$ is the scaled gain associated with the modulation of the curvature of the head.

The fixed points of Eqn 6 have direct behavioral relevance. In the absence of superposed temporal gradients [$\dot{\alpha}(t)=0$], the nonlinear oscillator described by Eqn 6 has two stable fixed points at $\theta^*=0,\pi$, which correspond to the two stable isothermal tracks in different directions but orthogonal to the spatial thermal gradient (Fig. 6C). With shallow superposed temporal gradients ($0 \ll \dot{\alpha}(t) \ll 1$), the two attractor points move over time, and, if $\dot{\alpha}(t)$ is oscillatory, the worm will be driven in floral trajectories as the fixed points oscillate over time. As the superposed temporal gradient approaches the magnitude of the temporal variations driven by self-motion ($\dot{\alpha}(t) \rightarrow 1$) the two fixed-points merge, so that θ^* is allowed to slide through successive cycles of 2π , and the worm may be driven in looping trajectories. A convenient visualization of motile behavior in spatiotemporal thermal gradients, within the context of our phenomenological model, is a parametric plot of the fixed point $\bar{\theta}^*$ and the 'driving force' $\dot{\alpha}(t)$ (Fig. 6D, Fig. 7E,F). In conclusion, the phenomenology of *C. elegans* navigating a variety of spatiotemporal thermal gradients can be qualitatively and quantitatively reconciled within the parameter space of a nonlinear dynamical system that describes the sensorimotor transformation for isothermal tracking.

Discussion

The ability of *C. elegans* to track isotherms in spatial thermal gradients has long been regarded as a

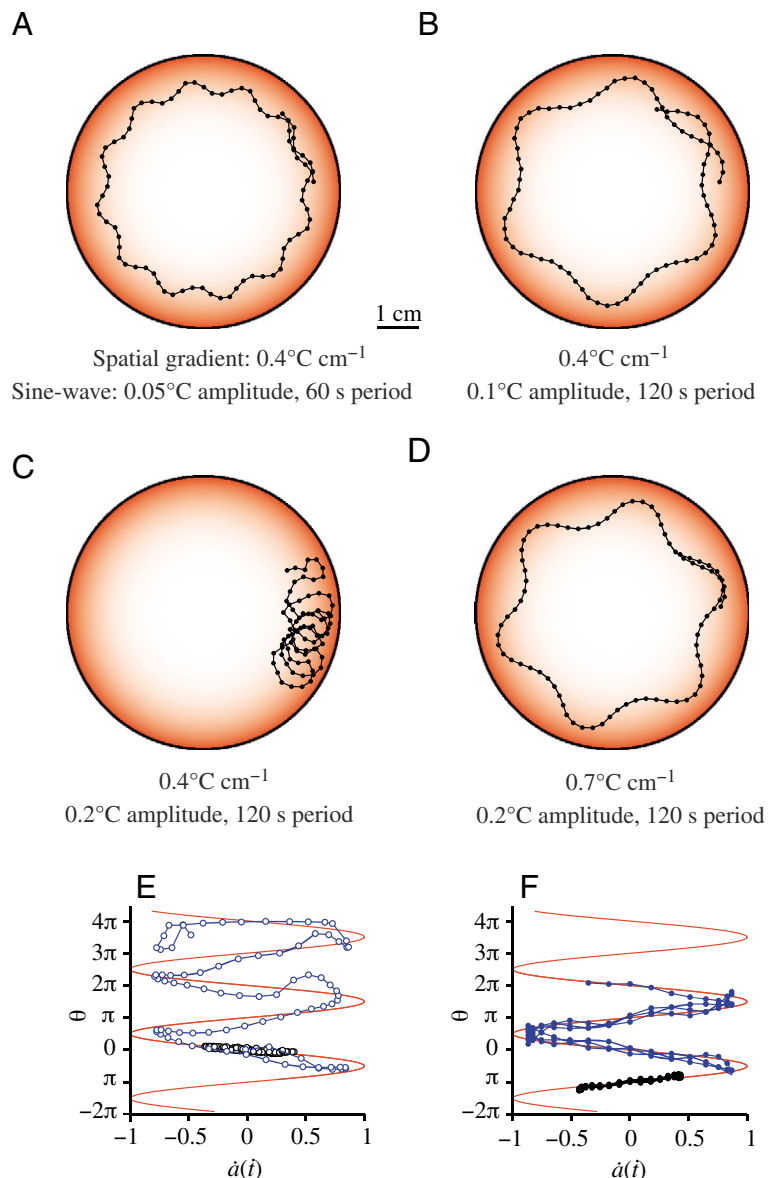


Fig. 7. Comparison of the model with experimental results. (A–D) Calculated trajectories of simulated worms using Eqn 2 and Eqn 3 and the same parameters of spatiotemporal thermal gradient as the experiments shown in Fig. 5 (E,F). The movements of real and simulated *C. elegans* responding to spatiotemporal thermal gradients are plotted as in Fig. 6D. The solid red line indicates the prediction of the model, $\bar{\theta}^*$, while the connected points correspond to the crawling trajectories exhibited real *C. elegans* (E) and calculated trajectories for simulated *C. elegans* (F) on a gradient of $0.4^\circ\text{C cm}^{-1}$. In each graph, black points correspond to superposed sine-wave temporal thermal gradients with 0.1°C amplitude and 120 s period (Fig. 5B and Fig. 7B), and the blue points correspond to superposed sine-wave temporal thermal gradients with 0.2°C amplitude and 120 s (data taken from Fig. 5C and Fig. 7C). The larger amplitude oscillation allows the trajectories to move to different branches, creating the looped trajectories observed in experiment and simulation. The isothermal tracking performance of real *C. elegans* and simulated *C. elegans* may be quantified by the r.m.s. deviation between the direction of forward movement and the instantaneous direction of the isotherm. For the flowerlike (black) trajectories of E and F the r.m.s. deviation for real and simulated *C. elegans* is 6° and 10° , respectively. For the looping (blue) trajectories of E and F, the r.m.s. deviation is 34° and 22° , respectively.

striking example of precise and deterministic navigation in a simple animal (Hedgcock and Russell, 1975). However, the underlying principles of sensorimotor control that produce the ability to track isotherms have not been examined. Here, we report that a simple and direct sensorimotor link – between a sensor of thermosensory input at the head and an effector that changes the curvature of the trajectory beginning at the head – explains not only the ability of *C. elegans* to maintain isothermal alignment in fixed spatial thermal gradients, but also the more complex trajectories of *C. elegans* navigating spatiotemporal thermal gradients.

We found that the mathematical conciseness of describing forward crawling in *C. elegans*, which may be approximated using the time-varying curvature of the animal's head propelled at constant speed, admits the development of a minimal phenomenological model of the sensorimotor transformation for isothermal tracking. We had only to augment the description of forward crawling with a behavioral rule by which *C. elegans* changes the curvature of its forward undulatory movement in response to changes in thermosensory input. We found that the resulting model provides a compact and accurate description of isothermal tracking behavior that is consistent with behavior across a wide range of spatiotemporal thermal gradients.

A complete understanding of the neurobiology of *C. elegans* isothermal tracking will require bridging our descriptive model of behavior with mechanistic models of nervous system operation. To date, the contributions of specific neurons to *C. elegans* thermotactic behavior have largely been described in qualitative terms – ablating individual neurons, such as the AFD sensory neurons or the AIY and AIZ interneurons, may abolish isothermal tracking behavior at temperatures near its previous cultivation temperature or abolish cryophilic movement at temperatures above its previous cultivation temperature, suggesting their general contribution to these behaviors (Mori and Ohshima, 1995; Chung et al., 2006). Progress will require defining the computational properties of the nervous system during the processing of behaviorally relevant thermosensory input. Once the physiological properties of the neural circuit for isothermal tracking are defined, it should be possible to build mechanistic neural network models that encode the basic operations of isothermal tracking behavior. Our descriptive model, as it fits the isothermal tracking behavior across a wide range of spatiotemporal thermal gradients, may provide a guide for developing such mechanistic models.

The sensorimotor strategy that gives rise to isothermal tracking deserves comparison with the sensorimotor strategy that enables *C. elegans* to exhibit cryophilic movement. One difference is that the two different behaviors are exhibited in different temperature ranges: the worm executes the strategy for isothermal tracking in a temperature range within 2°C of the previous cultivation temperature, and that for cryophilic movement in a temperature range above the previous cultivation temperature (Hedgcock and Russell, 1975; Ryu and Samuel, 2002). Another difference is that cryophilic

movement involves a stochastic strategy and that isothermal tracking involves deterministic maintenance of isothermal alignment. However, an interesting similarity is that both strategies utilize temporal processing of thermosensory input to assess the orientation of the animal's movements with respect to the ambient spatial thermal gradient by exploiting those same movements. During cryophilic movement, *C. elegans* extends (shortens) periods of forward movement in response to decreasing (increasing) temperature, and thus effects a biased random walk towards colder temperatures (Ryu and Samuel, 2002). In the case of isothermal tracking, it is the side-to-side movements of the head in a spatial thermal gradient that drives the temporal variations in temperature that allow *C. elegans* to deterministically correct its isothermal alignment. Therefore, the sensorimotor transformations underlying cryophilic movement and for isothermal tracking have computational consequences, converting the scalar quantity of thermosensory input into the vector quantity of motility, either average velocity down thermal gradients during cryophilic movement or isothermal alignment during isothermal tracking.

Finally, our observations allow us to estimate the thermal sensitivity of *C. elegans* during isothermal tracking. If *C. elegans* tracks isotherms by detecting temperature changes coupled to its own side-to-side movements on gradients as shallow as $0.1^{\circ}\text{C cm}^{-1}$, then it must detect temperature changes as small as 0.005°C . *C. elegans* would then approach the champion thermosensory metazoan, a blind cave beetle that detects temperature changes as small as 0.001°C (Corbiere-Tichane and Loftus, 1983).

This work was supported by grants from the NSF (A.D.T.S., L.M. and D.A.C.), the Sloan Foundation and the McKnight Foundation (A.D.T.S.), and a Human Frontier Science Program cross-disciplinary fellowship (D.B.). We thank anonymous referees for their thoughtful suggestions in improving this manuscript.

References

- Bargmann, C. I. and Horvitz, H. R.** (1991). Chemosensory neurons with overlapping functions direct chemotaxis to multiple chemicals in *C. elegans*. *Neuron* **7**, 729-742.
- Biron, D., Shibuya, M., Gabel, C., Wasserman, S. M., Clark, D. A., Brown, A., Sengupta, P. and Samuel, A. D. T.** (2006). A diacylglycerol kinase modulates long-term thermotactic behavioral plasticity in *C. elegans*. *Nat. Neurosci.* In press.
- Brenner, S.** (1974). The genetics of *Caenorhabditis elegans*. *Genetics* **77**, 71-94.
- Cassata, G., Kagoshima, H., Andachi, Y., Kohara, Y., Durrenberger, M. B., Hall, D. H. and Burglin, T. R.** (2000). The LIM homeobox gene *ceh-14* confers thermosensory function to the AFD neurons in *Caenorhabditis elegans*. *Neuron* **25**, 587-597.
- Chalfie, M., Sulston, J. E., White, J. G., Southgate, E., Thomson, J. N. and Brenner, S.** (1985). The neural circuit for touch sensitivity in *Caenorhabditis elegans*. *J. Neurosci.* **5**, 956-964.
- Chung, S. H., Clark, D. A., Gabel, C. V., Mazur, E. and Samuel, A. D. T.** (2006). The role of the AFD neuron in *C. elegans* thermotaxis analyzed using femtosecond laser ablation. *BMC Neurosci.* **7**, 30.
- Clark, D. A., Biron, D., Sengupta, P. and Samuel, A. D. T.** (2006). The AFD sensory neurons encode multiple functions underlying thermotactic behavior in *Caenorhabditis elegans*. *J. Neurosci.* **26**, 7444-7451.

- Corbiere-Tichane, G. and Loftus, R.** (1983). Antennal thermal receptors of the cave beetle, *Speophyes lucidulus*. *J. Comp. Physiol.* **153**, 343-351.
- Crocker, J. C. and Grier, D. G.** (1996). Methods of digital video microscopy for colloidal studies. *J. Colloid Interface Sci.* **179**, 298-310.
- Gomez, M., De Castro, E., Guarin, E., Sasakura, H., Kuhara, A., Mori, I., Bartfai, T., Bargmann, C. I. and Nef, P.** (2001). Ca²⁺ signaling via the neuronal calcium sensor-1 regulates associative learning and memory in *C. elegans*. *Neuron* **30**, 241-248.
- Gray, J. M., Hill, J. J. and Bargmann, C. I.** (2005). A circuit for navigation in *Caenorhabditis elegans*. *Proc. Natl. Acad. Sci. USA* **102**, 3184-3191.
- Hedgecock, E. M. and Russell, R. L.** (1975). Normal and mutant thermotaxis in the nematode *Caenorhabditis elegans*. *Proc. Natl. Acad. Sci. USA* **72**, 4061-4065.
- Hobert, O., Mori, I., Yamashita, Y., Honda, H., Ohshima, Y., Lui, Y. and Ruvkun, G.** (1997). Regulation of interneuron function in the *C. elegans* thermoregulatory pathway by the *ttx-3* LIM homeobox gene. *Neuron* **19**, 345-357.
- Karbowski, J., Cronin, C. J., Seah, A., Mendel, J. E., Cleary, D. and Sternberg, P. W.** (2006). Conservation rules, their breakdown, and optimality in *Caenorhabditis* sinusoidal motion. *J. Theor. Biol.* **242**, 652-659.
- Mohri, A., Kodama, E., Kimura, K. D., Koike, M., Mizuno, T. and Mori, I.** (2005). Genetic control of temperature preference in the nematode *Caenorhabditis elegans*. *Genetics* **169**, 1437-1450.
- Mori, I. and Ohshima, Y.** (1995). Neural regulation of thermotaxis in *Caenorhabditis elegans*. *Nature* **376**, 344-348.
- Okochi, Y., Kimura, K. D., Ohta, A. and Mori, I.** (2005). Diverse regulation of sensory signaling by *C. elegans* nPKC-epsilon/eta TTX-4. *EMBO J.* **24**, 2127-2137.
- Perkins, L. A., Hedgecock, E. M., Thomson, J. N. and Cullotti, J. G.** (1986). Mutant sensory cilia in the nematode *Caenorhabditis elegans*. *Dev. Biol.* **117**, 456-487.
- Pierce-Shimomura, J. T., Morse, T. M. and Lockery, S. R.** (1999). The fundamental role of pirouettes in *Caenorhabditis elegans* chemotaxis. *J. Neurosci.* **19**, 9557-9569.
- Ryu, W. S. and Samuel, A. D. T.** (2002). Thermotaxis in *Caenorhabditis elegans* analyzed by measuring responses to defined thermal stimuli. *J. Neurosci.* **22**, 5727-5733.
- Satterlee, J. S., Sasakura, H., Kuhara, A., Berkeley, M., Mori, I. and Sengupta, P.** (2001). Specification of thermosensory neuron fate in *C. elegans* requires *ttx-1*, a homolog of orthodenticle/Otx. *Neuron* **31**, 943-956.
- Sulston, J. and Hodgkin, J.** (1988). Methods. In *The Nematode Caenorhabditis elegans* (ed. W. B. Wood), pp. 587-606. Cold Spring Harbor, NY: Cold Spring Harbor Press Inc.
- Tsalik, E. L. and Hobert, O.** (2003). Functional mapping of neurons that control locomotory behavior in *Caenorhabditis elegans*. *J. Neurobiol.* **56**, 178-197.
- Wakabayashi, T., Kitagawa, I. and Shingai, R.** (2004). Neurons regulating the duration of forward movement in *Caenorhabditis elegans*. *Neurosci. Res.* **50**, 103-111.
- White, J. G., Southgate, E., Thomson, J. N. and Brenner, S.** (1986). The structure of the nervous system of the nematode *C. elegans*. *Philos. Trans. R. Soc. Lond. B Biol. Sci.* **314**, 1-340.